Bull. Chem. Soc. Ethiop. **2018**, 32(1), 101-109. ISSN 1011-3924
© 2018 Chemical Society of Ethiopia and The Authors Printed in Ethiopia
DOI: https://dx.doi.org/10.4314/bcse.v32i1.9

SYNTHESIS, CHARACTERIZATION AND PHOTOCATALYTIC ACTIVITY OF $Mn_2O_3/Al_2O_3/Fe_2O_3$ NANOCOMPOSITE FOR DEGRADATION OF MALACHITE GREEN

Nejat Redwan Habib[1*], Abi M. Taddesse[2] and Ayalew Temesgen[3]

[1]Adama Science and Technology University, School of Applied Natural Science, Department of Chemistry, P.O. Box 1888, Adama, Ethiopia
[2]Haramaya University, College of Natural and Computational Sciences, Department of Chemistry, P.O. Box 138, Haramaya, Ethiopia
[3]University of Gondar, College of Natural and Computational Science, Department of Chemistry, P.O. Box 196, Gondar, Ethiopia

(Received February 28, 2017; Revised February 20, 2018; Accepted March 6, 2018)

ABSTRACT. A $Mn_2O_3/Al_2O_3/Fe_2O_3$ nanocomposite photocatalyst was prepared by a co-precipitation method. Flame atomic absorption spectroscopy (FAAS), Fourier transform infrared spectroscopy (FTIR), X-ray diffraction (XRD), scanning electron microscope (SEM), and UV–Vis diffuse absorption spectroscopy (UV–Vis DAS) were employed to study elemental composition, functional group identification, structure, morphology, and band gap of the as-synthesized nanocomposite. The highest photodegradation efficiency was recorded for the sample containing the 10/10/80 percentages composition of $Mn_2O_3/Al_2O_3/Fe_2O_3$, respectively. The average crystallite size calculated from XRD for this sample was 40 nm. UV-Vis diffuse absorbance of the sample showed strong absorption in visible region at 550 nm, which is comparable to Fe_2O_3 which has absorption at 563.6 nm. This confirmed that coupling with alumina and manganese oxide did not contribute to the band gap narrowing but to delay the electron-hole recombination as witnessed by the highest photodegradation efficiency.

KEY WORDS: Co-precipitation method, Nanocomposite, Photocatalyst, Photodegradation, Malachite green

INTRODUCTION

Malachite green (MG) dye is widely used as antifungal, anti-bacterial and anti-parasitical therapeutic agent in aquacultures and animal husbandry. Also, it is widely used as a direct dye for silk, jute, paper, leather, etc. It can also be used as a saturable absorber in dye lasers, or as a pH indicator between pH 0.2–1.8. It was classified as a Class II Health Hazard which shows toxic effects on kidney, liver, gill and gonads of aquatic animals. It causes irritation and even cancer in humans when inhaled or ingested [1]. For the removal of dye pollutants, traditional techniques (adsorption on activated carbon, ultrafiltration, reverse osmosis, coagulation by chemical agents, ion exchange on synthetic adsorbent resins, etc.) can generally be efficiently used. Nevertheless, they are non-destructive, since they just transfer organic compounds from water to another phase, thus causing secondary pollution [2].

Recent studies have shown that heterogeneous semiconductor photocatalysis can be an alternative to conventional methods for the removal of dye pollutants from water [3]. Heterogeneous photocatalytic oxidations performed with light irradiated semiconductors dispersions have been extensively investigated owing to their high efficiency to completely mineralize the harmful organic species to carbon dioxide and water [4]. It has been a promising method for the elimination of organic pollutants in water and atmosphere [5]. When semiconductors are illuminated with an appropriate radiation source, electron/hole pairs are produced with electrons promoted to the conduction band leaving behind positive holes in the

*Corresponding author. E-mail: nejat.redwan@astu.edu.et

valence band. The generated electron/hole pairs induce a complex series of reactions that can result in the complete degradation of organic pollutants such as dye adsorbed on the semiconductor surface [3]. Due to high photosensitivity and large band gap, TiO_2 and ZnO are known to be good photocatalysts for degradation of many organic pollutants. However, there are some drawbacks associated with these compounds, such as charge carrier recombination, which occurs within nanoseconds and the band edge absorption threshold does not allow the utilization of visible light [5, 6]. Iron oxide (Fe_2O_3) is a well-known *n*-type semiconductor which exists in nature in many forms in which hematite (α-Fe_2O_3) and maghemite (γ-Fe_2O_3) are two common iron oxides. (α-Fe_2O_3), has become a particularly attractive material in its abundance, low cost, most active and stable under ambient conditions and no toxicity. It is widely used as a support or sensor and its low band gap (2.2 eV) making it promising as catalysts for photochemical transformations [1, 7]. Even though; its poor charge transport properties still remains a handicap for photochemical transformation rate of organic pollutant degradation [8, 9].

There are earlier reports on the improvement of the electronic properties of hematite by introducing transition metal cations and aluminum [8]. Alumina (Al_2O_3) is the most convenient support for the catalyst employed in the oxidation reduction reaction. This is because of its high surface area, thermal stability and porous structure. Also, it greatly increases the degree of dispersion of the catalytically active constituents, hindering their grain growth and thus increasing the activity and durability of supported catalysts. On the other hand, the combination of transition metal oxides may result in modification in their thermal behavior, geometric structures and electronic properties that lead to changes in catalytic functions [8, 10]. Mn_2O_3 can be used as cheap, environmental friendly catalysts for removing carbon monoxide, organic pollutants and nitrogen oxide or as an oxygen storage component (OSC) for a three-way catalyst [11]. Manganese binary mixtures are active catalyst for inorganic pollutant conversion [12]. These interesting features of Al_2O_3 and Mn_2O_3 lead us to investigate the photocatalytic properties of ternary oxide with Fe_2O_3.

EXPERIMENTAL

Materials

Chemicals used were: manganese(II) chloride tetrahydrate ($MnCl_2{\cdot}4H_2O$, MW: 197.9 g/mol, Labmark), iron(III) chloride hexahydrate ($FeCl_3{\cdot}6H_2O$, MW: 270.30 g/mol, 99.0%, Loba chemie), aluminum chloride hexahydrate ($AlCl_3{\cdot}6H_2O$, MW: 241.43g/mol, 99.0%, Merck), (sodium hydroxide (NaOH, MW: 40 g/mol, 98%, Merck), malachite green ($C_{23}H_{25}N_2Cl$, MW: 364.50 g/mol, 90%, Blulux), niric acid (HNO_3, MW: 63.01 g/mol, 67-72%, Fine-chem limited), hydrochloric acid (HCl, MW: 36.46 g/mol, 37-38%, Fine-chem limited).

Preparation of powder samples

A 0.1 M of $Mn_2O_3/Al_2O_3/Fe_2O_3$ mixed oxide was synthesized by co-precipitation method from manganese(II) chloride tetrahydrate ($MnCl_2{\cdot}4H_2O$), aluminum chloride hexahydrate ($AlCl_3{\cdot}6H_2O$) and iron(III) chloride hexahydrate ($FeCl_3{\cdot}6H_2O$) in deionized water with 10, 10, 80; 5, 15, 80 and 5, 5, 90 percentage of Mn_2O_3, Al_2O_3 and Fe_2O_3, respectively. The hydroxides were precipitated by concentrated sodium hydroxide at pH 12. The products were collected by filtration, washed several times with deionized water and dried at 110 ^oC for 24 h in an electrical oven. The dried samples were calcined at 400 ^oC for 4 h [11, 13, 14].

Characterization of powder samples

X-ray diffraction measurement was carried out to determine the crystal phase composition and size of the nanocomposite. The sample was crushed to fine particles and analyzed by X-ray

diffractometer (Shimadzu, XRD-7000, X-ray diffractometer), equipped with Cu K_α radiation (λ = 0.15405 nm) at room temperature in the scan range 2θ between 10 and 90◦. The accelerating voltage of 40 kV and the emission current of 30 mA were used. The surface morphology was studied by using a scanning electron microscope (EVO 18 SEM). The optical property of the sample was investigated by the band gap energy determination using UV-Visible diffuse absorption. The powder sample was dissolved in hot methanol then the UV-Visible diffuse absorbance was recorded at 200-800 nm range using SP65 spectrophotometer. Fourier transform infrared spectrum (Bruker IFS 120M) was recorded at room temperature in the region 4000–400 cm^{-1} to determine the surface functional groups. 10 mg of sample was thoroughly mixed with 100 mg (dry mass) of KBr and crushed to a fine powder. A transparent disc was formed by applying a pressure in moisture free atmosphere. The elemental compositions of the as-synthesized powder were analyzed by flame atomic absorption spectrophotometer. 0.1 g of the as-synthesized powder was digested with conc. HNO_3 (7 mL), conc. HCl (4 mL) using acid digestion tube till clear solution appears. The samples were transferred to 50 mL volumetric flasks and brought to volume using deionized water. 1 mL of this solution was diluted further to 50 mL. Standard solutions of 1000 mg/L Fe, Al and Mn were prepared by dissolving $FeCl_3{\cdot}6H_2O$, $AlCl_3{\cdot}6H_2O$ and $MnCl_2{\cdot}4H_2O$ in de-ionized water, and series standard solutions were prepared to plot the calibration curves of the metals by appropriate dilution.

Photocatalytic properties

Photocatalytic activities of the as-prepared powder sample were evaluated by photodecomposition of malachite green in aqueous solution. The experiments were carried out in the presence of UV and Visible light irradiation with $Mn_2O_3/Al_2O_3/Fe_2O_3$ photocatalyst. For a typical photocatalytic experiment, 200 mg of the prepared catalysts was added to 100 mL of the 100 ppm MG in aqueous solution in 250 mL Pyrex glass beaker. Before illumination of the samples by UV/Visible radiations, the solution was magnetically stirred for 30 min in dark in order to establish adsorption desorption equilibrium. During the illumination stage, air/oxygen was purged into the solution with the help of a porous tube at hand purging in order to keep the suspension of the reaction homogenous. The suspension was irradiated by UV/Visible light source at 12 cm distance. At 30 min time intervals, about 10 mL aliquots were sampled, centrifuged at 4500 rpm, and filtered. The dye concentration in the filtrate was analyzed by measuring the absorption intensity of MG at 620 nm. The UV lamp with a definite power 12 W, 230 V and 50 Hz frequency was employed as UV light source and incandescent bulb was used as visible light source with a definite power of 40 W, 220 V and 60 Hz frequency. Percentage degradation of MG dye was calculated using the following relation:

$$\% \text{ Degradation} = \left(\frac{c_o - c_t}{c_o}\right)100 \quad (1)$$

where c_o is concentration of dye at initial stage; c_t is concentration of dye at time t.

RESULTS AND DISCUSSION

Elemental composition

The percentage of iron, aluminum and manganese in the as-synthesized samples were determined with the results as depicted in Table 1. The amount of each metal in the three different composites is in good agreement with the theoretical composition.

Table 1. Calculated Percentages of powder samples.

Sample code	% Mn[a]	% Mn[b]	% Fe[a]	% Fe[b]	% Al[a]	% Al[b]
A	10	9.9	80	76.3	10	9.9
B	5	4.8	80	76.3	15	14.8
C	5	4.8	90	89.5	5	4.8

[a]initial percentage composition of as-synthesized sample. [b]percentage composition of as-synthesized sample calculated from the FAAS.

X-Ray diffraction analysis

The average crystallite size (D) was calculated from XRD pattern according to the Scherrer equation: $D = \frac{k\lambda}{\beta\cos\theta}$ where, k is constant (about 0.9), λ is the wavelength (0.15405 nm), β is the full width at half maximum (FWHM) of the diffraction line and θ is the diffraction angle [15]. From the XRD data (Table 2) we see that the as-prepared sample is nanosized. From the as-synthesized ternary oxide samples, sample with (80% Fe, 10% Al and 10% Mn) was chosen which have the highest photodegradation efficiency and its crystallite size was found to be 40.52 nm. The XRD pattern of this sample is depicted in Figure 1. The XRD diffraction pattern of the nanocomposite in general appeared to be dominated by amorphous structure with limited crystalline domains. Accordingly, the peaks at 2θ values of 35.64° and 62.45° correspond to hematite (α-Fe_2O_3) phase [96-900-0140] where as the peak at 2θ value of 31° could be associated with maghemite phase (γ-Fe_2O_3) [06-900-6317]. The additional peak observed at 2θ values of 45.11 shows the presence of bixbyite (α-Mn_2O_3) [96-151-4107]. The reason for the absence of peaks related to Al_2O_3 could be its low percentage (10%) in the composite and relatively lower calcinations temperature employed in our experiment (400 °C). In fact, crystallized alumina such as γ-Al_2O_3 might be present under thermal treatment at 800 °C and α-Al_2O_3 might present under thermal treatment at 1000 °C [9, 16, 17].

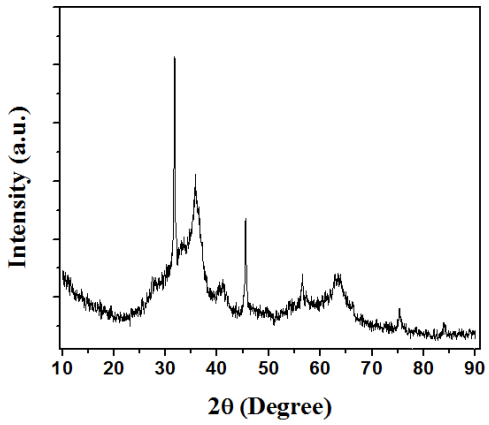

Figure 1. The XRD patterns of samples with 10, 10, 80 $Mn_2O_3/Al_2O_3/Fe_2O_3$ percentage composition, respectively.

Table 2. Average crystallite size (D) of the as prepared nanocomposite photocatalysts calcined at 400 ^oC for 4 h.

Percentage (%) composition Fe	Al	Mn	2θ (Degree)	β (Radian)	D (nm)
80	10	10	31.75	0.223	40.52
80	15	5	33.34	0.371	22.38
90	5	5	33.42	0.269	30.87

Morphology investigation

Figure 2 shows the SEM images of ternary $Mn_2O_3/Al_2O_3/Fe_2O_3$ nanocomposite with different magnifications. In lower magnification the aggregated morphology of the nanocomposite is shown. At higher magnification the image specifies rod like structures of the host Fe_2O_3 particles. The addition of aluminum and manganese oxide may influence the size and morphology of pure Fe_2O_3.

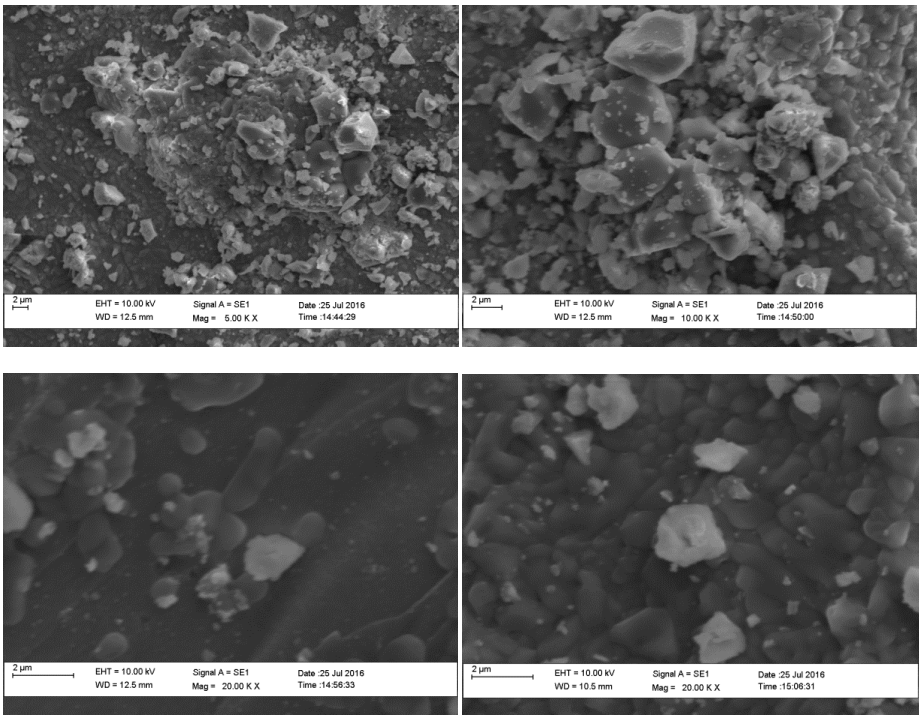

Figure 2. SEM micrographs of sample with 10, 10, 80 $Mn_2O_3/Al_2O_3/Fe_2O_3$ percentage composition respectively with 2 µm resolution.

FT-IR analysis

The peak at 3430 cm^{-1} is attributable to the O–H stretching vibration of water and an $^-$OH group on the surface of photocatalyst. Hydroxyl groups are crucial to the photocatalytic reactions since they can react with photoexcited holes generated on the catalyst surface and produce hydroxyl

radicals, which act as powerful oxidants [9]. The band at 1628 cm^{-1} might be attributed to O-H bending vibrations; the bands at 1385 and 1124 cm^{-1} are characteristic absorption band of Al_2O_3 [18]. The bands at 480 and 570 cm^{-1} could represent the M-O vibrational mode of the nanocomposite [19].

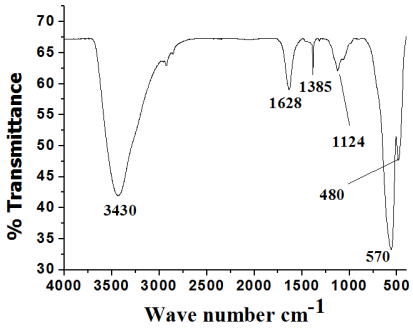

Figure 3. FT-IR data of sample with 10, 10, 80 $Mn_2O_3/Al_2O_3/Fe_2O_3$ percentage composition, respectively.

UV-Visible diffuse absorption analysis

The band gap of the catalyst directly affects photocatalytic activity in such a way that, the direct absorption of band-gap photons would result in the generation of electron-hole pairs within the catalysts, subsequently; the charge carriers began to diffuse to the surface of the catalysts. As a result, the photocatalytic activity for decomposing organic compounds with catalyst might be enhanced [20]. The wavelengths of the absorption edges in the UV-Vis spectra were determined by plotting a vertical line from the apex of the curve [21]. From the absorption spectra, it has been investigated that the absorbance of the as-prepared nanocomposite photocatalyst is about ~540 nm, as shown in Figure 4. The measured band gap was found to be 2.29 eV, according to the following formula [22].

$$E_g(eV) = \frac{1240}{\lambda_{max}} \quad (2)$$

where, λ_{max} = 540 nm, $E_g(eV) = \frac{1240}{540}$ = 2.29 eV. This value indicates that the as-prepared photocatalyst is sensitive to visible portion of the solar spectrum.

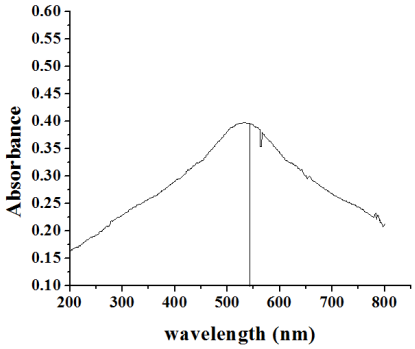

Figure 4. UV-Visible absorption spectra of sample with 10, 10, 80 $Mn_2O_3/Al_2O_3/Fe_2O_3$ percentage composition, respectively.

Photodegradation of malachite green

The photodecomposition of malachite green dye was done for a total of 180 min under UV and visible light irradiation as shown in Figures 5 and 6. Sample with (80% Fe, 10% Al and 10% Mn) showed the highest photoactivity which was 98%; samples with (90% Fe, 5% Al and 5% Mn) and with (80% Fe, 15% Al and 5% Mn) showed 97 and 92% decomposition, respectively, in visible light. The percent decomposition of the target dye is found to be 72%, 75% and 49% for samples A (80% Fe, 10% Al and 10% Mn), B (90% Fe, 5% Al and 5% Mn) and C (80% Fe, 15% Al and 5% Mn), respectively, in the presence of UV light, as presented in Table 3.

Remarkable degradation was observed in visible light. This was a positive result for the as prepared nanocomposite. The increased degradation in the presence of visible light was due to the unequal number of d electrons in the 3d orbital of Fe and Mn when Fe^{3+} was replaced by Mn^{3+}, since they have the same ionic radii in their high spin state, which is 0.645 Å [23, 24]. This is very important, since the electron mobility plays a key role in photocatalysis and this is one of the problems that prevent hematite from being an efficient photocatalyst [8].

The visible light degradation results of all samples showed only slight differences. This is because Fe_2O_3 acts as a host in all the samples by taking minimum amount of 80% and the percentage of Mn_2O_3 and Al_2O_3 changes slightly from 5 to 15%. As observed from degradation results, increasing Mn_2O_3 and alumina contents from 5 to 10%, increased photocatalytic activity from 97 to 98%. A decrease in degradation was observed when alumina content was increased from 10 to 15%. Samples A and B show similar degradation with slight increase in degradation of sample A under UV light irradiation. A noticeable difference was observed in degradation result of sample C which contains the lower fraction of alumina from all as-prepared samples. Increasing alumina content from 5 to 15% increases the degradation under UV light.

Table 3. Percentage photodecomposition of malachite green dye under visible and UV-light irradiation.

Sample code	Percentage (%) composition			% decomposition under visible light	% decomposition under UV light
	Fe	Al	Mn		
A	80	10	10	98	72
B	80	15	5	92	75
C	90	5	5	97	49

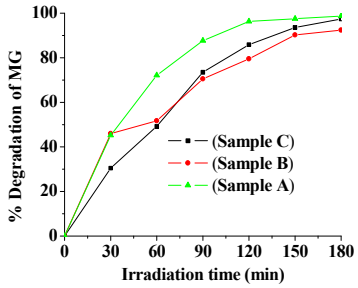

Figure 5. Plots of percentage degradation of malachite green dye as function of time under visible light irradiation.

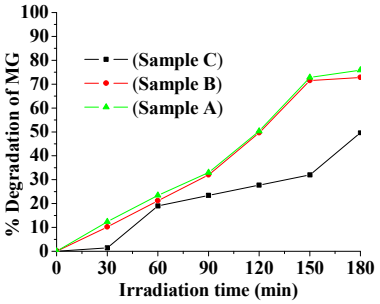

Figure 6. Plots of percentage degradation of malachite green dye as function of time under UV light irradiation

CONCLUSION

A $Mn_2O_3/Al_2O_3/Fe_2O_3$ nanocomposite with different percentages was prepared by co-precipitation method. FAAS analysis showed that the obtained percentages of iron, aluminum and manganese were similar to the calculated composition. The highest photodegradation was observed for sample 80% Fe, 10% Al and 10% Mn, in the visible region. The FT-IR spectrum for this sample shows the presence functional groups attributable to metal oxides. The XRD results revealed that the as prepared sample is nanosized and its strong peaks show the presence of hematite, maghemite and bixbyite. Rod like structure of the host particle Fe_2O_3 was shown in SEM micrographs. The UV-Vis diffuse reflectance spectra measured band gap was found to be 2.29 eV. This value indicates that the as-prepared photocatalyst is amenable for the phtocatalytic experiment carried under visible light domain.

ACKNOWLEDGMENTS

The authors would like to thank University of Gondar (Department of Chemistry), Adama Science and Technology University (Department of Chemistry), Addis Ababa University (Department of Chemistry) for technical support and Ministry of Education, Ethiopia for providing the financial support to accomplish this work.

REFERENCES

1. Pawar, M.; Khajone, A.J. Photodegradation of malachite green dye over sol-gel synthesized nanocrystalline α-Fe_2O_3. *Chem. Pharm. Res.* **2012**, 4, 1880-1884.
2. Konstantinou, K.I.; Albanis, A.T. TiO_2-assisted photocatalytic degradation of azo dyes in aqueous solution: Kinetic and mechanistic investigations: A review. *Appl. Catal. B: Environ.* **2004**, 49, 1-14.
3. Welderfael, T.; Yadav, P.O.; Taddesse, M.A.; Kaushal, J. Synthesis, characterization and photocatalytic activities of Ag-N-Codoped ZnO nanoparticles for degradation of methyl red. *Bull. Chem. Soc. Ethiop.* **2013**, 27, 221-232.
4. Elaziouti; Laouedj, N.; Ahmed, B. ZnO-Assisted photocatalytic degradation of congo red and benzopurpurine 4B in aqueous solution. *J. Chem. Eng. Process Technol.* **2011**, 2, 1-9.
5. Pawar, J.M.; Khajone, D.A.; Gaoner, D.M.; Chandel, S.P. Photodegradation of malachite green dye over sol-gel synthesized nanocrystalline *α*-Fe_2O_3. *Int. J. Adv. Sci. Res. Technol.* **2012**, 2, 471-476.

6. Guesh, K.; López-Muñoz, J.M.; Márquez-Álvarez, C.; Chebude, Y.; Diaz, I. Ethiopian natural zeolites for photocatalysis. *Bull. Chem. Soc. Ethiop.* **2015**, 29, 431-440.
7. Carabineiro, C.A.S.; Bogdanchikov, N.; Tavares, B.P.; Figueiredo, L.J. Nanostructured iron oxide catalysts with gold for the oxidation of carbon monoxide. *RSC Advances* **2012**, 2, 2957-2965.
8. Praveen, S.C.; Timon, V.; Valant, M. Electronic band gaps of ternary corundum solid solutions from Fe_2O_3–Cr_2O_3–Al_2O_3 system for photocatalytic applications: A theoretical study. *Comput. Mater. Sci.* **2012**, 55, 192-198.
9. Li, B.F.; Li, Z.X.; Liu, S.C.; Liu, X.T. Effect of alumina on photocatalytic activity of iron oxides for bisphenol A degradation. *J. Hazard. Mater.* **2007**, 149, 199-207.
10. Shaheen, M.W.; Hong, S.K. Thermal characterization and physiochemical properties of Fe_2O_3-Mn_2O_3/Al_2O_3 system. *Thermochim. Acta* **2002**, 381, 153-164.
11. Gnanam, S.; Rajendran, V. Synthesis of CeO_2 or α-Mn_2O_3 nanoparticles via sol–gel process and their optical properties. *J. Sol-Gel Sci. Technol.* **2011**, 58, 62-69.
12. Carabineiro, A.S.; Fernandes, B.F.; Vital, S.J.; Ramos, M.A.; Fonseca, M.I. N_2O conversion using manganese binary mixtures supported on activated carbon. *Appl. Catal. B: Environ.* **2005**, 59, 181–186.
13. Abdulkadir, I.; Babando, A.A. Some wet routes for synthesis of hematite nanostructures. *Afr. J. Pure Appl. Chem.* **2013**, 7, 114-121.
14. Battiston, S.; Rigo, C.; Severo, da C.E.; Mazutti, A.M.; Kuhn, C.R, Gündel A.; Foletto, L.E. Synthesis of zinc aluminate ($ZnAl_2O_4$) spinel and its application as photocatalyst. *Mater. Res.* **2014**, 17, 734-738.
15. Mebrahtu, C.; Taddesse, M.A.; Goro, G.; Yohannes, T. Natural pigment sensitized solar cells based on ZnO-TiO_2-Fe_2O_3 nanocomposite in quasi-solid state electrolyte system. *Bull. Chem. Soc. Ethiop.* **2017**, 31, 263-279.
16. Abebe, B.; Taddesse, M.A.; Kebede, T.; Teju, E.; Diaz, I. Fe-Al-Mn ternary oxide nanosorbent: Synthesis, characterization and phosphate sorption property. *J. Environ. Chem. Eng.* **2017**, 5, 1330-1340.
17. Taddesse, M.A.; Tesfahun, T.K.; Tofik, S.A.; Girma, G.G. Fe–Al binary oxide nanosorbent: Synthesis, characterization and phosphate sorption property. *J. Environ. Chem. Eng.* **2016**, 4, 2458-2468.
18. Ghezelbash, Z.; Ashouri, D.; Mousavlan, S.; Ghandi, A.H.; Rahama, Y. Surface modified Al_2O_3 in fluorinated polyimide/Al_2O_3 nanocomposites: Synthesis and characterization. *Bull. Mater. Sci.* **2012**, 35, 925-931.
19. Woo, K.; Lee, J.H.; Ahn, J.-P.; Park, S.Y. Sol–gel mediated synthesis of Fe_2O_3 nanorods. *Adv. Mater.* **2003**, 15, 1761-1764.
20. Luan, J.; Hu, Z. Synthesis, property characterization, and photocatalytic activity of novel visible light-responsive photocatalyst Fe_2BiSbO_7. *Int. J. Photoenergy* **2012**, 2012, 1-11.
21. Wanga, C.; Xua, B.-Q.; Zhaoc, J. Preparation and photocatalytic activity of ZnO/TiO_2/SnO_2 mixture. *J. Solid State Chem.* **2005**, 178, 3500-3506.
22. Rahman, M.M.; Gruner, G.; Al-Ghamdi, S.M.; Daous, A.M.; Khan, B.S.; Asiri, M.A. Chemo-sensors development based on low-dimensional codoped Mn_2O_3-ZnO nanoparticles using flat-silver electrodes. *Chem. Cent. J.* **2013**, 7, 60.
23. Baazaoui, M.; Zemni; Boudard, M.; Rahmouni, H.; Gasmi, A.; Selmi, A. Dumezzine, M. Magnetic and electrical behaviour of La0.67Ba0.33Mn1-x$Fex O_3$ perovskites. *Int. J. Nanoelectron. Mater.* **2010**, 3, 23-36.
24. Laha, S.; Natarajan, S.; Gopalakrishnan, J.; Morán, E.; Sáez-Puche, R.; Alario-Franco, M.Á.; Dos Santos-Garcia, A.J.; Pérez-Flores' J.C.; Kuhn, A.; García-Alvarado, F. *Phys. Chem.* **2015**, 17, 3749-3760.